

MALAYSIAN JOURNAL OF ANALYTICAL SCIENCES



Journal homepage: https://mjas.analis.com.my/

Research Article

Influence of crosslinker and monomer concentration on the swelling behaviour and morphological characteristics of hemicellulose-based hydrogels from oil palm empty fruit bunches

Sabiha Hanim Saleh^{1,2*}, Nur Syafiqah Antashah Azaha¹, Nurul Asyikin Abd Halim¹, Shariff Ibrahim^{1,2}, Mohammed Falalu Hamza¹, Noraini Hamzah^{1,2}

¹School of Chemistry and Environment, Faculty of Applied Sciences, Universiti Teknologi MARA, 40450 Shah Alam, Selangor, Malaysia

²Industrial Waste Conversion Technology Research Group, Faculty of Applied Sciences, Universiti Teknologi MARA, 40450 Shah Alam, Selangor, Malaysia

*Corresponding author: sabihahanim@uitm.edu.my

Received: 19 September 2024; Revised: 28 June 2025; Accepted: 2 July 2025; Published: 22 August 2025

Abstract

This study investigates the extraction of hemicellulose from oil palm empty fruit bunches (OPEFB) and its subsequent use in the synthesis of hemicellulose-based nanocomposite hydrogels. Given the limited understanding of how the crosslinker and monomer concentration affect the properties of these hydrogels, further exploration is essential. Six distinct hydrogels were synthesised by varying the amounts of the crosslinker N,N'-methylenebisacrylamide (MBA) and the monomer acrylic acid (AA). The primary aim was to evaluate the impact of these variations on the swelling behaviour of the hydrogels. Hemicellulose extraction was performed using a microwave-assisted alkaline solution at 130 °C for 30 min, and the extracted hemicellulose was then utilised to prepare the hydrogels. Swelling studies indicated that the hydrogel with 0.5% MBA exhibited the highest swelling percentage at 1008%, while the optimal monomer concentration of 20% achieved a swelling percentage of 1933%. Fourier Transform infrared spectroscopy identified key functional groups, including O-H, C≡C, C=O, and C-O stretches, reflecting differences in crosslinker and monomer concentrations. Field emission scanning electron microscopy analysis revealed distinct surface morphologies influenced by both crosslinker and monomer concentrations. Hydrogels with lower MBA (0.1%) and moderate AA (20%) exhibited rougher, more open surfaces, while higher MBA (1.0%) and AA (22%) contents resulted in smoother, denser structures. The optimal swelling performance was observed in samples with 0.5% MBA and 20% AA, corresponding to a well-balanced network structure. These findings highlight the critical need to optimise the crosslinker-to-monomer ratio and the concentrations of these components to develop hydrogels with desirable swelling properties and structural characteristics.

Keywords: crosslinker, monomer, oil palm empty fruit bunches, hydrogel, hemicellulose

Introduction

This research explores the extraction of hemicellulose from oil palm empty fruit bunches (OPEFB) and its use in synthesising hemicellulose-based nano composite hydrogels. OPEFB, a by-product from oil palm trees predominantly cultivated in Malaysia, Thailand, Indonesia, and other regions, is recognised as an economical natural fibre due to its advantageous properties and abundance in Malaysia [1]. For example, hemicellulose hydrogels can be produced from OPEFB, which contains significant amounts of hemicellulose suitable for hydrogel production. In recent years, the production of hemicellulose

hydrogels using OPEFB as a sustainable feedstock has gained attention. Besides OPEFB, hemicellulose-rich materials include agricultural residues such as corn cobs [2], rice straw [3], wheat straw [4], sugarcane bagasse [5], and pineapple peels [6].

Hemicellulose, a vital class of natural polymers following cellulose, has not yet been fully exploited for its potential as an eco-friendly raw material. These non-cellulosic heteropolysaccharides consist of short-branched chains with various sugar units (hexose and pentose) arranged in different proportions and substituents. Hemicellulose, found in plant cell walls,

forms strong bonds with cellulose microfibrils through hydrogen bonds and van der Waals forces hemicellulose [7,8]. Generally, comprises heterogeneous group of plant-derived polysaccharides, including D-xylose, D-mannose, Dgalactose, L-arabinose, D-galactose, and 4-O-methyl-D-glucuronic acid. Due to its renewability, biodegradability, and biocompatibility, hemicellulose is widely utilised in gel material preparation (hydrogel). Hydrogels are polymeric materials with a three-dimensional network structure, typically formed by the physical or chemical crosslinking of long-chain hydrophilic polymers that can absorb water and swell. This crosslinking process enhances the hydrogel's stability and mechanical strength, allowing it to retain its shape and integrity when exposed to water or other solvents. Additionally, crosslinking influences the hydrogel's swelling capacity, porosity, biocompatibility. Hydrogels made from hemicellulose and crosslinkers have diverse applications in fields such as biomedicine, tissue engineering, and drug delivery.

Current research on bio-based hydrogels for various applications has faced limitations in optimising the balance between water absorption and structural integrity. Inadequate crosslinking in the polymer network leads to poor mechanical properties, while too much crosslinking reduces the hydrogel's ability to absorb water. There is a need for further investigation into how varying monomer and crosslinker concentrations can be fine-tuned to achieve optimal swelling behaviour and mechanical strength. This study focuses on the production of hemicellulose-based hydrogels derived from OPEFB. In this research, acrylic acid (AA) was used as the monomer, and N,N'-methylenebisacrylamide (MBA) served as the crosslinker in hydrogel preparation. The objectives were to assess the effect of crosslinker and monomer concentrations on the swelling behaviour of hemicellulose-based hydrogels and to investigate their physical and chemical properties. The characterisation of the hydrogels was carried out using Fourier transform infrared (FTIR) spectroscopy, field emission scanning electron microscopy (FESEM), and swelling analysis [6,9,10].

Materials and Methods Materials

Fresh empty fruit bunches (EFB) were collected from local palm oil plantations in Shah Alam. Distilled water and an alkaline solution of sodium hydroxide (NaOH) were used for initial processing. The pH was adjusted using hydrochloric acid (HCl), and hemicellulose was precipitated by the addition of 95% ethanol (Systerm), which facilitated the separation of the solid fraction from the solution. For hydrogel synthesis, acrylic acid (AA, 99%, Sigma-Aldrich) was

used as the monomer, while N,N-methylenebisacrylamide (MBA, 99%, Chemiz) served as the crosslinking agent. A redox initiation system consisting of sodium sulphite (Na₂SO₃, 99.3%, Bendosen) and potassium persulphate (K₂S₂O₈, 99.0%, Chemiz) was employed to initiate the polymerisation reaction.

Preparation of oil palm empty fruit bunches

After the extraction of oil, the OPEFB were soaked in water for 24 h and rinsed with tap water to remove any remaining oil and dirt. The OPEFB were then left to dry at room temperature for 24 h. Prior to extraction, the dried OPEFB were ground and sieved to achieve a particle size of $60 \ \mu m \ [11]$.

Microwave-assisted alkaline extraction

Microwave-assisted extraction was conducted using the ETHOS EASY microwave system equipped with a rotor containing 15 PTFE-TFM containers, each with a 100 mL capacity (SK-15 rotor, Milestone, Sorisole, Italy). This system adheres to industry standards, such as US EPA 3015, 3051, and 3052. With certain modifications, NaOH served as the solvent in the alkaline extraction process to extract hemicellulose from the EFB. A pressure vessel was prepared by mixing 3 g of dried EFB with a predetermined amount of NaOH to achieve a loading ratio of 15 mL NaOH per gram of dry biomass. Hemicellulose extraction was conducted under the following parameters: temperature (130 °C), duration (30 min), and NaOH concentration (10% w/v). The sample mixture was then filtered to separate the filtrate from the solid residue. To precipitate the dissolved hemicellulose, 4 L of 95% ethanol was added to the filtrate after it was neutralised to a pH of 5.5 using 6 M HCl. The precipitated hemicellulose was subsequently separated by centrifugation (4,500 rpm, 15 min), freeze-dried, and properly labelled.

Preparation of hemicellulose-based hydrogel

To prepare the hydrogel, 0.5g of purified hemicellulose was dissolved in 10 mL of distilled water in a beaker. The mixture was stirred and heated in a water bath at 90 °C for 1 h. A redox initiator system consisting of 0.04 g of Na₂SO₃ and 0.01 g of K₂S₂O₈ was then added under magnetic stirring for 10 min. To investigate the effect of crosslinker content, varying amounts of MBA at 0.1%, 0.5%, and 1.0% (w/v) were added to the mixture, while maintaining a constant AA concentration of 22% (v/v). In a separate set of samples, the AA concentration was varied at 17%, 20%, and 22% (v/v) with a fixed MBA concentration of 0.5% (w/v) to study the effect of monomer content. All percentages of MBA and AA were calculated based on the amount of hemicellulose dissolved in the 10 mL solution. After the addition of MBA and AA, the reaction proceeded for 1–2 h in the water bath at 90 °C. The resulting hydrogels were then dried in a vacuum dryer at 40 °C until a constant weight was achieved.

Characterisation of hydrogel Swelling analysis

A portion of the hydrogel was immersed in distilled water to initiate the swelling process at room temperature (25 °C) for 48 h. Once the swelling equilibrium was reached, the swelling ratio (SR) was calculated using Equation (1) [9].

$$S = \frac{W_t - W_d}{W_d} \times 100\% \tag{1}$$

Where W_d is the initial weight of the dried hydrogel (g) and W_t is the weight of the hydrogel after swelling (g).

Fourier transform infrared spectroscopy analysis

FTIR spectroscopy was employed to identify the functional groups within the hydrogel, providing insights into its chemical composition and molecular structure. For this analysis, both the potassium bromide and hydrogel samples were ground into a fine powder using an agate mortar after complete drying. The resulting mixture was uniformly applied onto a tablet and scanned by the infrared spectrometer over a range of 400–4000 cm⁻¹ [6,10].

Field emission scanning electron microscopy analysis

FESEM analysis was conducted on hydrogel samples that had undergone swelling in a solution, followed by vacuum freeze-drying for 48 h to examine the surface morphology [12]. To prepare the hydrogel samples for FESEM, a small section of the freeze-dried hydrogel was attached to the sample holder using double-sided adhesive material.

Results and Discussion Swelling analysis

Table 1 shows the SR for hydrogels with different quantities of MBA as a crosslinker. The hydrogel with 0.1% crosslinker exhibits a swelling percentage of 576%. This value is lower than that of the hydrogel with 0.5% crosslinker, despite its substantial SR. This indicates that insufficient crosslinking results in a less stable network, which may not support optimal water absorption [13]. The hydrogel with 0.5% crosslinker achieves the highest swelling percentage of 1008%. This indicates an optimal crosslinker density, providing a balance between network density and

water absorption capacity [9]. The hydrogel with 1.0 g of crosslinker demonstrates a lower swelling percentage of 546%. This suggests that excessive crosslinking creates a denser network that restricts water uptake compared to the hydrogel with 0.5% crosslinker [14]. The SR is highest for the hydrogel with 0.5% crosslinker, reinforcing that this concentration supports the optimal network structure for water absorption. Lower SRs for both 0.1% and 1.0% crosslinker quantities highlight that both insufficient and excessive crosslinking impair the hydrogel's swelling ability [15]. These results underscore the importance of precise crosslinker concentration in hydrogel synthesis. The 0.5% crosslinker quantity appears to be optimal, achieving a balance between network structure and swelling capacity [9,16].

Based on the swelling behaviour of hydrogels with different monomer concentrations, as shown in Table 2, it is evident that the quantity of monomers significantly influences the hydrogel's capacity to absorb water. The hydrogel with 20% AA exhibits the highest SR of 19.33, corresponding to a swelling percentage of 1933%. This result suggests that at 20% AA, the hydrogel achieves an optimal balance between monomer concentration and crosslinking density, allowing for the formation of a wellstructured and interconnected polymer network that maximises water absorption [17]. Conversely, hydrogels with 17% AA and 22% AA show reduced swelling percentages of 1305% and 1008%, respectively. The hydrogel with 17% AA likely has a lower monomer concentration, resulting in a less dense network that restricts effective water absorption.

On the other hand, the hydrogel with 22% AA may have an excessively dense network due to the higher monomer content, which could limit the available space for water absorption and lead to decreased swelling [9]. These findings highlight the importance of optimising monomer concentration in hydrogel synthesis. Achieving the right balance is crucial for developing a hydrogel network structure that is well-connected, allowing for maximum swelling while avoiding an overly dense or insufficiently dense formation. This relationship between monomer quantity and hydrogel performance aligns with other studies that highlight the complex interplay among monomer concentration, crosslinking density, and the resulting hydrogel properties [16].

Table 1. Swelling ratios of hydrogels with different quantities of MBA (crosslinker)

MBA (%)	$W_d(g)$	$W_t(\mathbf{g})$	SR	Swelling (%)
0.1	11.2506	76.1420	5.76	576
0.5	5.4398	60.3080	10.08	1008
1.0	8.7066	56.2898	5.46	546

Table 2. Swelling ratios of hydrogels with different quantities of AA (monomer)

AA (%)	$W_d(\mathbf{g})$	$W_t(\mathbf{g})$	SR	Swelling (%)
17	3.9035	54.8600	13.05	1305
20	3.2228	65.5210	19.33	1933
22	4.7976	53.1712	10.08	1008

Fourier transform infrared spectroscopy

The FTIR spectra for hydrogels with different crosslinker concentrations are shown in Figure 1. For hydrogels with varying amounts of MBA (0.1%, 0.5%, and 1.0%), the O-H stretching vibrations were observed at 3259.59 cm⁻¹, 3271.25 cm⁻¹, and 3272.11 cm⁻¹. The broadness of these peaks indicates the presence of hydrogen bonding. Variations in peak positions may suggest differences in the bonding environment or hydrogen bonding the hydrogels contain Additionally, alkynes, characterised by a carbon-carbon triple bond (C≡C). The C≡C stretching vibrations were detected at 2130.03 cm⁻¹, 2162.49 cm⁻¹, and 2162.18 cm⁻¹, reflecting strong stretching vibrations at relatively high wavenumbers. The C=O stretching vibrations, associated with carbonyl groups, appeared at 1634.61 cm⁻¹, 1632.41 cm⁻¹, and 1632.81 cm⁻¹. Hydrogen bonding can influence these C=O stretching vibrations, potentially causing shifts in peak positions. The broad peaks further suggest hydrogen bonding involvement. The C-O stretching vibrations, indicative of ether groups within the hydrogel, were observed at 1044.58 cm⁻¹, 1048.45 cm⁻¹, and 1050.10 cm⁻¹ [18].

The FTIR spectra for hydrogels with different AA concentrations (17%, 20%, and 22%) are shown in Figure 2. The O-H stretching vibrations appeared at 3372.43 cm⁻¹, 3372.62 cm⁻¹, and 3373.42 cm⁻¹, representing hydroxyl groups in the hydrogel. Variations in these peak positions may be due to different chemical environments or hydrogen bonding strengths affecting the vibrational frequency of the O-H groups. The C-H stretching vibrations were observed at 2932.17 cm⁻¹, 2920.35 cm⁻¹, and 2920.55 cm⁻¹, reflecting the vibrational stretching of carbonhydrogen bonds. C≡C stretching vibrations were detected at 2162.91 cm⁻¹, 2162.85 cm⁻¹, and 2161.04 cm⁻¹, attributed to the stronger triple bonds requiring more energy to stretch. C=C stretching vibrations, indicative of alkenes, were observed at 1684.30 cm⁻¹, 1686.22 cm⁻¹, and 1686.15 cm⁻¹, suggesting the presence of carbon-carbon double bonds and unsaturated hydrocarbons. Finally, C-O stretching vibrations, representing ether groups, were seen at 976.40 cm⁻¹, 976.42 cm⁻¹, and 976.41 cm⁻¹ [18].

Field emission scanning electron microscopy

Figure 3((a)–(c)) illustrates the surface morphology of hydrogels synthesised with different amounts of MBA (0.1%, 0.5%, and 1.0%), highlighting the impact of crosslinking density on hydrogel structure. Hydrogel with 0.1% MBA (Figure 3(a)) shows a highly rough and cracked surface with visible microstructural irregularities. Although clearly defined pores are not observed, the disrupted surface suggests a loosely crosslinked, fragile network. This structure may offer a larger free volume for water absorption; however, the low SR of 5.76 (576%), as shown in Table 1, indicates that the network may be mechanically unstable or prone to collapse upon water uptake, limiting its swelling capacity. This suggests that the low crosslinker concentration leads to an insufficiently connected network, resulting in a structure with numerous surface irregularities. Such a poorly formed network could hinder water retention and swelling, as demonstrated in other studies [15].

In contrast, the hydrogel with 0.5% MBA (Figure **3(b)**) displays a smoother and more uniform surface, suggesting a well-balanced and cohesive polymer network. Although distinct pores are not visible, the morphology indicates an optimal crosslinking density that enables the hydrogel to swell effectively without structural collapse. This is supported by the highest SR of 10.08 (1008%), as recorded in **Table 1**, confirming that a moderate amount of crosslinker facilitates the formation of an ideal network for water retention. The improved swelling performance is likely due to enhanced network integrity, consistent with the findings reported by Chen et al. [9]. In Figure 3(c), the hydrogel with 1.0% MBA becomes very smooth and compact, showing minimal roughness or cracking. This morphology reflects a densely crosslinked structure that restricts network expansion and water uptake. As anticipated, the SR drops to 5.46 (546%), supporting the understanding that excessive

crosslinking limits free volume and reduces hydrogel swelling performance. When a hydrogel contains an excessive amount of crosslinker, it forms a dense and rigid network structure. However, this reduces the internal free volume available for water absorption, resulting in lower swelling capacity. This outcome is supported by findings in other studies [19, 20]. These observations highlight the importance of balancing crosslinker concentration to achieve desirable hydrogel properties. Insufficient crosslinking results in a weak structure, whereas excessive crosslinking produces a dense network that restricts swelling. Although distinct porosity is not apparent under FESEM, variations in surface roughness and morphological features still offer valuable insights into the internal network. The hydrogel containing 0.5% MBA represents the ideal balance, providing a well-formed network that is structurally sound and capable of significant swelling.

Figure 4((a)-(c)) presents the FESEM images of

hydrogels synthesised with different concentrations of AA at a fixed crosslinker content (0.5% MBA). These surface morphologies show significant changes as the AA content increases and are correlated with the swelling behaviour shown in Table 2. In Figure 4(a) (17% AA), the hydrogel surface appears relatively smooth, compact, and tightly packed, with some visible cracks. This ordered structure suggests a denser network with limited free volume, likely due to significant shrinkage during drying [21]. The relatively low degree of surface irregularity is consistent with a moderate SR of 13.05 (1305%), suggesting limited water uptake capacity due to the more constrained polymer network. With an increased AA content of 20%, as seen in Figure 4(b), the surface becomes noticeably rough and irregular, featuring deep grooves and loose fibre-like structures. These features are indicative of a more open surface structure and suggest increased apparent porosity, potentially due to a more loosely crosslinked network [22].

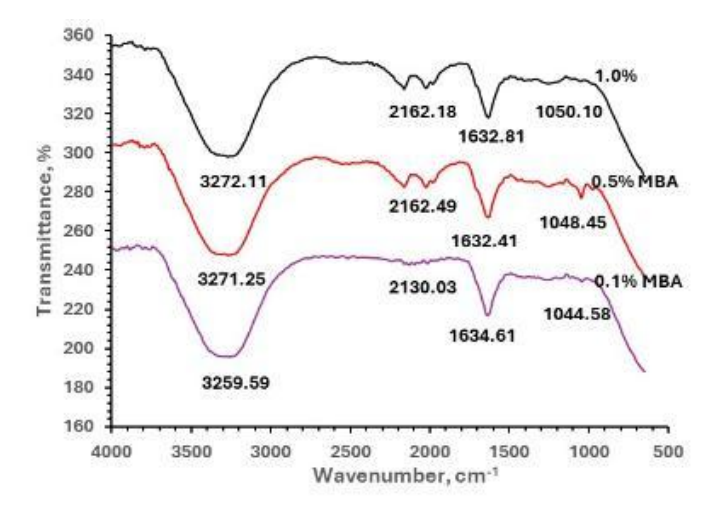


Figure 1. FTIR spectra of hydrogels using different MBA percentages

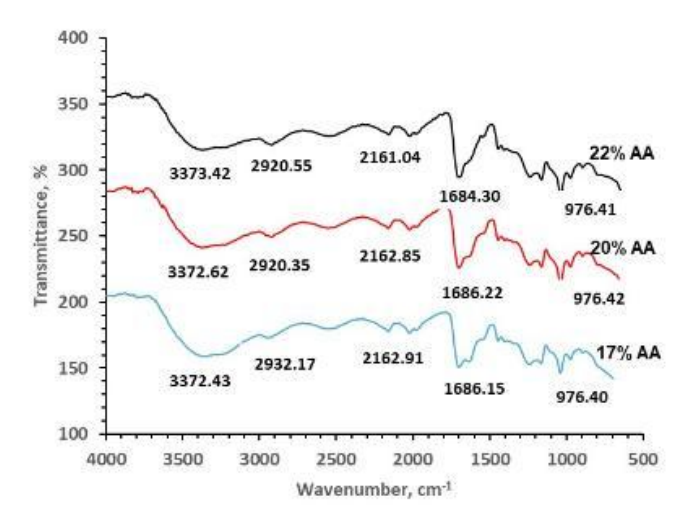


Figure 2. FTIR spectra of hydrogels using different AA percentages

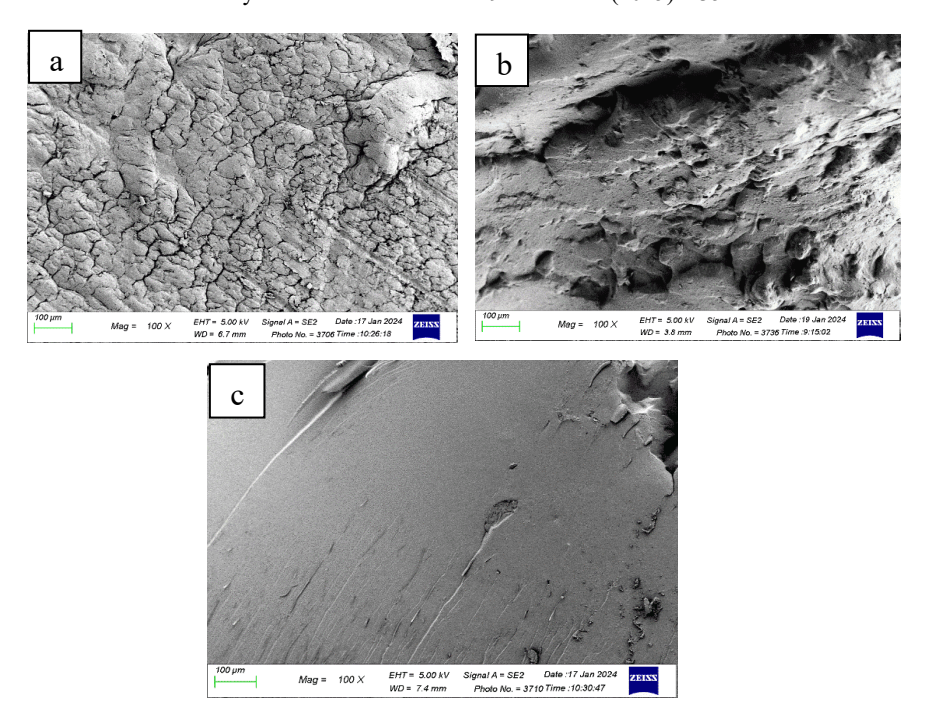


Figure 3. FESEM images of a) 0.1% MBA, b) 0.5% MBA, and c) 1.0% MBA at 100x magnification

This morphological change facilitates greater water diffusion and retention within the hydrogel, which is confirmed by the highest SR of 19.33 (1933%) among the samples. This implies that at this concentration, the network structure is optimally balanced to promote both fluid uptake and network integrity. In Figure 4(c) (22% AA), the surface exhibits a smoother, denser morphology with fewer cracks and a more consolidated structure. No visible pores are observed in the FESEM image, and the compact surface

appearance suggests a restricted ability for water to penetrate the hydrogel matrix. Correspondingly, the SR shows a notable decrease to 10.08 (1008%) compared to 20% AA. This reduction may be due to the high monomer concentration, which could lead to excessive crosslinking or network compaction, thereby limiting water absorption. Although the surface appears well-formed, the dense internal structure likely hinders the hydrogel's ability to swell effectively.

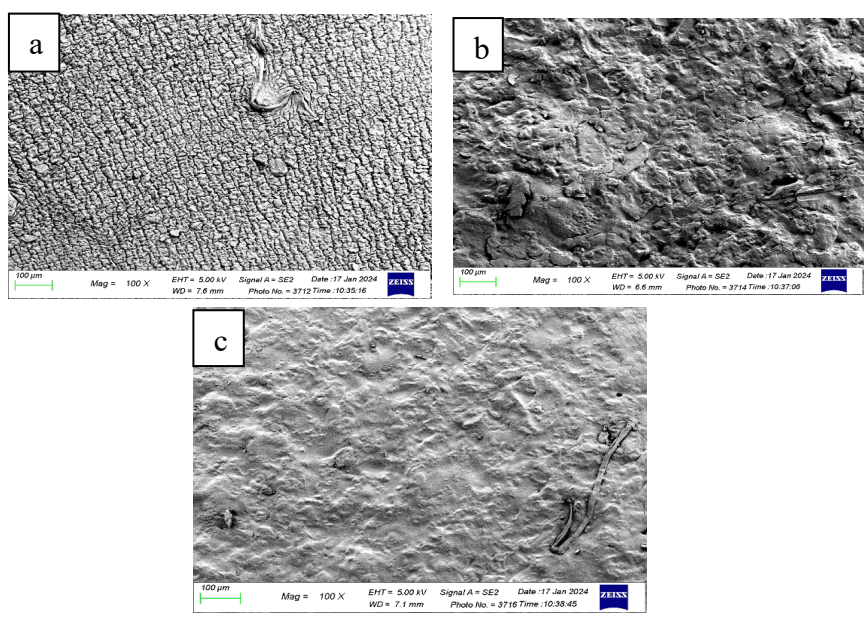


Figure 4. FESEM images of a) 17% AA, b) 20% AA, and c) 22% AA at 100x magnification

Conclusion

The study revealed that the hydrogel achieved maximum swelling (1008%) at an optimal crosslinking density of 0.5%. Swelling decreased when the MBA amount was 0.1% or 1.0%, highlighting the importance of maintaining a balanced crosslinker ratio. Similarly, the highest swelling percentage (1933%) was observed with 20% AA while keeping the MBA constant at 0.5%. Deviations from this monomer quantity, either 22% AA or 17% AA, resulted in reduced swelling, underscoring the impact of monomer concentration on hydrogel performance. Achieving the optimal hydrogel structure requires precise optimisation of both the crosslinker-to-monomer ratio and the quantities of these components. The FTIR analysis identified functional groups such as O-H, C≡C, C=O, and C-O, with their peak positions varying according to the crosslinker and monomer amounts. The surface morphology of hydrogels varied notably with different crosslinker and monomer concentrations. Lower MBA (0.1%) and moderate AA (20%) levels produced rougher, more open surfaces, while higher concentrations of MBA (1.0%) or AA (22%) resulted in smoother, more compact structures. In conclusion, the study demonstrates that the swelling capacity and structural properties of hydrogels strongly depend on achieving the right balance between crosslinker and monomer.

Acknowledgement

The authors are grateful to the Ministry of Higher Education for the financial support provided for this research with grant number FRGS/1/2022/STG04/UITM/02/10.

References

- 1. Padzil, F. N. M., Lee, S. H., Ainun, Z. M. A., Lee, C. H., and Abdullah, L. C. (2020). Potential of oil palm empty fruit bunch resources in nanocellulose hydrogel production for versatile applications: A review. *Materials*, 13(5): 1245.
- Puitel, A.C., Balan, C.D. and Nechita, M.T. (2025). Corn stalks-derived hemicellulosic polysaccharides: Extraction and purification. *Polysaccharides*, 6(2): 1-19.
- 3. Zulyadi, N. H., Saleh, S. H., and Sarijo, S. H. (2016). Fractionation of hemicellulose from rice straw by alkaline extraction and ethanol precipitation. *Malaysian Journal of Analytical Sciences*, 20(2): 329-334.
- 4. Rodríguez-Sanz, A., Fuciños, C., Torrado, A. M., and Rúa, M. L. (2022). Extraction of the wheat straw hemicellulose fraction assisted by

- commercial endo-xylanases. Role of the accessory enzyme activities. *Industrial Crops and Products*, 179: 114655.
- Zhang, L., Huang, H., He, T., Sun, J., Chen, K., and Yue, F. (2024). Highly selective extraction of lignin and hemicellulose with retained original structure from sugarcane bagasse via low-temperature soaking and acidic precipitation. *Industrial Crops and Products*, 209: 118015.
- Mad Zahir, N. A. A., Hamzah, N., Mohd Zaki, H., Ibrahim, S., and Saleh, S. H. (2021). Optimisation of microwave-assisted water extraction of pineapple peel hemicellulose using response surface methodology. *Malaysian Journal of Analytical Sciences*, 25 (6): 1095-1106.
- 7. Liu, K., Du, H., Zheng, T., Liu, H., Zhang, M., Zhang, R., Li, H., Xie, H., Zhang, X., Ma, M., and Si, C. (2021). Recent advances in cellulose and its derivatives for oilfield applications. *Carbohydrate Polymers*, 259: 117740.
- 8. Liu, W., Du, H., Zhang, M., Liu, K., Liu, H., Xie, H., Zhang, X., and Si, C. (2020). Bacterial cellulose-based composite scaffolds for biomedical applications: A review. *ACS Sustainable Chemistry & Engineering*, 8(20): 7536-7562.
- 9. Chen, T., Liu, H., Dong, C., An, Y., Liu, J., Li, J., Li, X., Si, C., and Zhang, M. (2020). Synthesis and characterization of temperature/pH dual sensitive hemicellulose-based hydrogels fromeucalyptus APMP waste liquor. *Carbohydrate Polymers*, 247: 116717.
- 10. Shahzamani, M., Taheri, S., Roghanizad, A., Naseri, N., and Dinari, M. (2020). Preparation and characterization of hydrogel nanocomposite based on nanocellulose and acrylic acid in the presence of urea. *International Journal of Biological Macromolecules*, 147:187-193.
- 11. Weerasooriya, P. R. D., Nadhilah, R., Owolabi, F. A. T., Hashim, R., Abdul Khalil, H. P. S., Syahariza, Z. A., Hussin, M. H., Hiziroglu, S., and Haafiz, M. K. M. (2020). Exploring the properties of hemicellulose based carboxymethyl cellulose film as a potential green packaging. *Current Research in Green and Sustainable Chemistry*, 1-2: 20-28.
- 12. Aljeboree, A. M., Hasan, I. T., Al-Warthan, A., and Alkaim, A. F. (2024). Preparation of sodium alginate-based SA-g-poly(ITA-co-VBS)/RC hydrogel nanocomposites: And their application towards dye adsorption. *Arabian Journal of Chemistry*, 17(3): 105589.
- 13. Singh, J. and Dhaliwal, A. (2018). Synthesis, characterization and swelling behavior of

- silver nanoparticles containing superabsorbent based on grafted copolymer of polyacrylic acid/Guar gum. *Vacuum*, 157: 51-60.
- Nasution, H., Harahap, H., Dalimunthe, N.F., Ginting, M.H.S., Jaafar, M., Tan, O.O.H., Aruan, H.K. and Herfananda A. L. (2022). Hydrogel and effects of crosslinking agent on cellulose-based hydrogels: A review. *Gels*, 8(568): 1-31.
- Soares, P. A., de Seixas, J. R., Albuquerque, P. B., Santos, G. R., Mourao, P. A., Barros, W., Jr., Correia, M. T., and Carneiro-da-Cunha, M. G. (2015). Development and characterization of a new hydrogel based on galactomannan and kappa-carrageenan. *Carbohydrate Polymers*, 134: 673-679.
- Peng, F., Guan, Y., Zhang, B., Bian, J., Ren, J. L., Yao, C. L., and Sun, R. C. (2014). Synthesis and properties of hemicelluloses-based semi-IPN hydrogels. *International Journal of Biological Macromolecules*, 65: 564-572.
- Ninciuleanu, C.M., Ianchiş, R., Alexandrescu, E., Mihăescu, C.I., Scomoroşcenco, C., Nistor, C.L., Preda, S., Petcu, C. and Teodorescu, M. (2021). The effects of monomer, crosslinking agent, and filler concentrations on the viscoelastic and swelling properties of poly(methacrylic acid) hydrogels: A comparison. *Materials*, 14(9): 2305.
- Banerjee, S., Patti, A. F., Ranganathan, V., and Arora, A. (2019). Hemicellulose based biorefinery from pineapple peel waste: Xylan extraction and its conversion into xylooligosaccharides. *Food and Bioproducts Processing*, 117: 38-50.
- 19. Lambrecht, S., Schröter, H., Pohle, H., and Jopp, S. (2024). Swelling behavior of novel hydrogels produced from glucose-based ionic monomers with varying cross-linkers. *ACS Omega*, 9: 5418-5428.
- Shin, S., Kim, S., Hong, S., Kim, N., Kang, J., and Jeong, J. (2025). Tuning the swelling behavior of superabsorbent hydrogels with a branched poly(aspartic acid) crosslinker. *Gels*, 11(3): 161.
- Groult, S., Buwalda, S., and Budtova, T. (2021). Pectin hydrogels, aerogels, cryogels and xerogels: Influence of drying on structural and release properties. European Polymer Journal, 149: 110386.
- Yang, J., Liang, G., Xiang, T., and Situ, W. (2021). Effect of crosslinking processing on the chemical structure and biocompatibility of a chitosan-based hydrogel. *Food Chemistry*, 354: 129476.